JJMIE

Volume 18, Number 4, December. 2024
ISSN 1995-6665
Pages 795- 810
https://doi.org/10.59038/jjmie/180412
Editor-in-Chief: Prof. Ali M. Jawarneh

Jordan Journal of Mechanical and Industrial Engineering

A Multi Fuzzy-based Variable Step Size P&O MPPT Algorithm for PV Systems

Assem Alkarasneh[1*], Khaled Bataineh[2], Yusra Aburmaileh[3]

[1]Department of Mechanical Engineering, Faculty of Engineering Technology, Al-Balqa Applied University, Jordan
[2] Department of Mechanical Engineering, Jordan University of Science and Technology, Jordan
[3] Department of Engineering and Artificial Intelligence, Al-Salt Technical College, Al-Balqa Applied University, Jordan

Received 1 Jul 2024 Accepted 11 Sep 2024

Abstract

Photovoltaic (PV) system transforms sunlight into electricity. PV cells have non-linear I-V relationships with one point producing the maximum power output from the PV cells. The best efficiency is obtained at the maximum power point (MPP) of PV system. This paper proposes a hybrid MPP control strategy that incorporates both fuzzy logic controller (FLC) and the Perturbation and Observation (P&O) algorithm under various cases of whether conditions. The proposed algorithm is continuously searching for maximum power point and modify it as needed under rapidly changing weather conditions (irradiance and temperature) and be able to perform successful tracking of the MPP under partially shaded conditions. The performance and the power output of the system will be evaluated using simulation under specific weather conditions. The developed controller is implemented in two stages to overcome the drawbacks of the conventional P&O algorithm; the first stage uses fuzzy controller to provide an initial guess for P&O where it combines the speed of FLC approximation with the accuracy of P&O. The second stage uses another fuzzy controller to find a proper step size of P&O to enhance the transient response and reduce the steady-state oscillations. The results show that the efficiency of the proposed remains high under various scenarios; Uniform irradiation, sudden irradiation, partial shading (weak, moderate, and strong). Furthermore, results demonstrated that the proposed hybrid FLC-P&O can effectively improve the accuracy of the conventional P&O algorithm.

Keywords: A hybrid MPPT controller; FUZZY-P&O; Partial shading; Photovoltaic; Boost converter.

Nomenclature

Symbol	Definition	Unit
PV	Photovoltaic	-
MPP	Maximum Power Point	-
FLC	Fuzzy Logic Controller	-
P&O	Perturbation And Observation	-
DC	Direct Current	-
MPPT	Maximum Power Point Tracker	-
IC	Incremental Conductance	-
FOCV	Fractional Open-Circuit Voltage	-
FSCC	Fractional Short-Circuit Current	-
PID	Proportional Integral Derivative	-
HC	Hill Climbing	-
NN	Neural Network	-
PSO	Particle Swarm Optimization	-
ABC	Artificial Bee Colony	-
MOSFET	A Metal–Oxide–Silicon Field-Effect Transistor	-
PWM	Pulse Width Modulation	-
I_L	Photocurrent	Ampere
I_{ph}	Photocurrent	Ampere
V	Output Voltage	Volt
ID	Parallel Diode Current	Ampere
R_{sh}	Shunt (Parallel) Resistance	Ohme
I_{sh}	Shunt Current	Ampere
R_s	Series Resistance	Ohme
I	Output Current	Ampere
G	Irradiance	W/m^2
Tc	Operating Cell Temperature	K
$T_{c,ref}$	Cell Temperature at STC = 25 + 273 = 298	K
I_{sc}	Short Circuit Current At STC.	Ampere
α_{Isc}	Coefficient Temperature of I_{sc} = 0.05% For Proposed PV Module.	Ampere/K
I_{rs}	Diode Reverse Saturation Current	Ampere
ε_G	Physical Band Gap Energy, (1.12 Ev for Si).	eV
k	Boltzmann Constant 1.38x10^{-23}	J/K.
q	Charge Of Electron 1.602x10^{-19}	C
N_s	Number Cells Connected in Series,60 Cells.	-
A	Ideality Factor, Which Is 1.2 For Si-Mono.	-
R_L	Load Resistance	Ohme
R_{MPP}	Ideal Internal Resistance of PV Array At MPP	Ohme
d_{mpp}	Duty Cycle of The Converter at Maximum Power Point MPP	-
V_O	Output Voltage	Volt
Po	Output Power	W
ΔIpv	Input Current Ripple	Ampere
ΔV_O	output voltage ripple	Volt
L	Inductor Value	mH
V_{MMP}	Voltage at Maximum Power Point MPP	Volt
I_{MMP}	Current at Maximum Power Point MPP	Ampere
C_1	Input Capacitor	µF
C_2	Output Capacitor	µF
fs	Switching Frequency	kHz
P_{max}	Maximum Value of Real Power	W
Voc	Open Circuit Voltage	Volt
Isc	Short Circuit Current	Ampere
LMPP	Local Maximum Power Point	W
GMPP	global maximum power point	W

* Corresponding author e-mail: assemalkarasneh@bau.edu.jo.

1. Introduction

Renewable energy technology has gained huge attention from researchers and scientists due to the energy crisis and they are focusing on increasing the performance of solar cells and investigating novel uses in order to greatly increase the production and use of clean energy [1], [2], [3], [4], [5], [6], [7]. PV systems exploit solar energy to supply green renewable power, it is used as an alternative of the electricity produced from conventional fossil fuels. Solar cell/PV system transforms sunlight into electricity where this electrical energy can supply various systems, such as: hydrogen production, electrical power systems, water-pumping systems, etc. The generated power relies on irradiance amount, temperature, and other weather conditions. The maximum power point (MPP) of the module depends on the radiation, therefor, MPP tracking is essential to obtain and maintain maximum power levels. Utilizing DC-DC convertors, PVs are being controlled by the algorithm to provide the maximum power to the load.

Enhancing the electrical energy of PV cells or the converter's efficiency is difficult, as it relies on the available modern technology. Accordingly, improving the efficiency of the MPPT algorithm by new control strategies is easy and not expensive, which increases the PV power generation [8]. This leads to a huge improvement on MPPT algorithms, for the direct methods: perturbation and observation (P&O) [9], [10], Incremental Conductance (IC) [11], Fractional Open-Circuit Voltage (FOCV) [12], Fractional Short-Circuit Current (FSCC) [13], Hill Climbing (HC) [14], and bond graph algorithm[15]. The conventional methods have some disadvantages such as, large oscillations, trapped in local peaks slow convergence and inaccuracy. In order to eliminate these problems, numerous revisions were implemented on these traditional methods and indirect methods that integrated the conventional direct methods with more advanced strategies: perturbation and observation (PID-P&O)[16],[17], PID-incremental conductance [18], fuzzy logic-perturbation and observation (FLC-P&O) [19], [20] and fuzzy logic-hill climbing (FLC-HC) [21], , others that use artificial intelligence neural network (NN) [22], [23], fuzzy logic [24],[25], genetic algorithms (GA) [26], [27], particle swarm optimization (PSO) [28], artificial bee colony algorithm (ABC) [29], ...etc. The P&O method is a nonlinear method for MPPT, which compares prior power amount to current ones to obtain the MPP, utilizing the duty cycle as a variable [30], This method is the most common one used in commercial products [31]. Meanwhile, it has some drawbacks; Oscillating around maximum power point and utilizing a fixed step size. Low values of step size leading small fluctuations throughout steady-state weather conditions with slow response. Otherwise, larger step size leading faster response with higher oscillations. Various developments on the conventional P&O method have been presented to enhance its performance under various weather conditions. By all of the artificial intelligent controllers, FLC is the easiest one to integrate with other algorithms' structures. Recently, researchers have paid a great attention to FLC because of their ability to provides better results than other traditional controllers and improve performance in intricate systems, particularly in t he field of robotics transportation systems, industrial contr ol, and renewable systems [32], [33], [34], [35]. A Modified P&O-Fuzzy MPPT variable step size has been proposed in order to overcome some drawbacks according to the conventional P&O MPPT method to enhance the transient response and reduce the steady-state oscillations [36], [37]. The results showed that the conventional P&O and the modified one had a difference in tracking efficiency of 0.38% for the modified P&O.

This study aims to develop an efficient MPPT method that overcomes the drawbacks of the conventional methods under various cases of whether conditions. The system is implemented in two stages, the first one uses fuzzy controller to provide an initial guess for P&O and the second one uses another fuzzy controller to find a proper step size of P&O. The efficiency of the proposed study is studied successfully using MATLAB/Simulink. The system is studied in various scenarios; Uniform irradiation, sudden irradiation, and partial shading (weak, moderate, and strong). A comparative study between the fixed and variable step size P&O algorithms are studied and it confirms that the proposed system can effectively improve the accuracy compared to the fixed step size algorithm. The rest of this paper is organized as the following: Section 2 presents the PV modeling. The hybrid variable step size P&O MPPT controller is proposed in Section 3. While Section 4 discusses the simulation results. Finally, Section 5 concludes the study and gives the perspectives future works.

2. Methods

2.1. PV Cell Modeling

The basic structure of a solar panel cell is a p-n semiconductor junction. DC current is generated when the device is exposed to light. The light irradiance affects the produced current. The solar cell's equivalent electric circuit is considered as a current source which is connected in parallel with the diode and shunt resistance R_{SH}. A resistance R_S is connected in series in the electric circuit, as presented in Figure 1. The PV solar panel is classified into two categories based on the number of diodes, which are the single-diode model and two-diode model. The solar cell single-diode model is well-known and extensively used for evaluation and estimation the output PV current I. Because of its simplicity and accuracy the single diode model was considered in this proposed study [38]. This model is shown below on Figure 1.

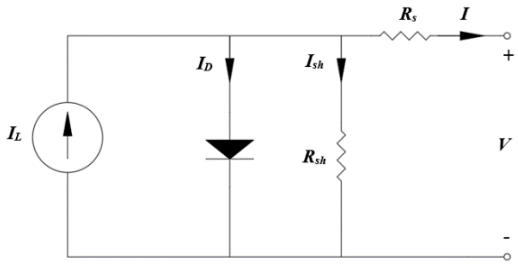

Figure 1. The Solar cell single-diode model.

The PV output current can be calculated from the well-known Shockley diode equation:

$$I = I_{ph} - I_s\left[e^{\left(\frac{q(V+I.R_s)}{A.N_s.V_T}\right)} - 1\right] - \left(\frac{V+IR_S}{R_{sh}}\right) \quad (1)$$

The saturation current of the PV cell is expressed by:

$$I_s = I_{rs}\left(\frac{T_{op}}{T_{ref}}\right)^3\left[e^{\left(\frac{-q\varepsilon_G}{A.k}\left(\frac{1}{T_{op}}-\frac{1}{T_{ref}}\right)\right)}\right] \quad (2)$$

The reversed saturation current and the photon current of PV solar panel are given by equation 3 and 4, respectively.

$$I_{rs} = \frac{I_{sc}}{\left[e^{\left(\frac{Voc}{A.N_s.V_T}\right)}-1\right]} \quad (3)$$

$$I_{ph} = \left(\frac{G}{1000}\right)\left(I_{sc}+\alpha_{I_{sc}}\cdot\Delta T\right) \quad (4)$$

Where:
$\Delta T = Tc\text{-}T_{c,ref}$ (Kelvin).

2.2. Maximum Power Point Tracker (MPPT) Techniques

MPPT is a significant concern in PV solar systems which is defined as a set of rules (automatic control algorithm) that is utilized as part of a charge controllers used for extracting and achieving maximum available possible power harvest from PV solar system array during instantaneous changes in light intensity, shading level, temperature value, and solar module specifications and characteristics. So, the major goal of MPPT techniques is to track the maximum power point of the PV solar panel. MPPT affects by both changing in temperature and radiation. With many changeable temperature and solar radiation, the MPP also varies. The maximum power point tracker is a DC-DC converter that connected between the PV solar units and the inverter or battery. So, the MPPT is utilized to adjust the electric power yield by increasing or decreasing the output power under the demanded system's requirements. There are abundant MPPT techniques that have been studied, implemented, optimized and developed by researchers [39], [40], [41]. Maximum power point refers to maximum output current and maximum output voltage at which a PV solar module can generate the maximum power value or peak power. Solar radiation, ambient temperature, and solar cell temperature all affect the value of maximum power. Typical PV module provides electric power with maximum output voltage of around 17 V when estimated at a cell temperature of 25°C. According to the weather condition the value of the output voltage will change. It will fall to about 15 V on a very hot climate, and it will also rise to 18 V on a very cold climate.

2.3. Boost Converter Model

In this study, a boost converter was utilized to convey the energy from the PV units to the load resistance and it's interfaced between the PV solar unit and resistor load in an MPPT system. The DC-DC Converter is a type of electronic devices that alters electrical power from one voltage level to another according to the duty cycle (d) [42]. The correct design of the DC–DC converter is essential to guarantee that the PV solar system is working at the best value of the efficiency, according to the requirement. In this proposed work, a boost converter was selected to modify and step up the input voltage and control the level of output power to the load. The components of the boost converter circuit are namely, resistor (R), inductor (L), Capacitor(C), switching device, and a diode. as demonstrated in Figure 2. In this investigation, a metal–oxide–silicon field-effect transistor (MOSFET) and stand power diode are chosen since there are commonly used for low to moderate electric power applications [43]. The frequency of the switching device is specified at 25 kHz after the balancing between the switching losses and size of inductor.

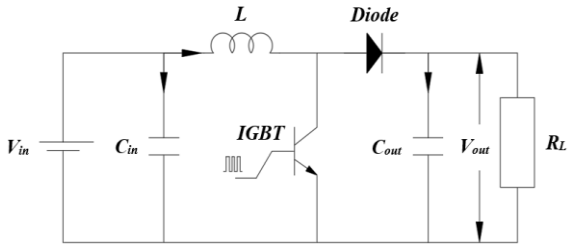

Figure 2. Circuit diagram of the Boost converter.

The input voltage is determined by the PV solar panels output, and the fluctuation of converter duty cycle value is executed in accordance with the output of the MPPT. The running of DC-DC boost converter primarily depends on the opening and closing of the switching device, to insert the charging and discharging statuses, respectively [44]. The term duty cycle (d) is defined as the ratio between the input voltage and output voltage, and it is given by Equation (5). This variable is controlled by a PWM signal generator, which is in turn controlled by a physical device which in this case is a metal–oxide–silicon field-effect transistor (MOSFET). For the continuous conduction mode, the value of d was constrained between 0 and 1.

$$V_{out} = \frac{V_{in}}{1-d} \quad (5)$$

The other components of the boost converter are selected as the following:

- Selection of the resistor:

The following equation describes the relationship between the load resistance (R_L) of boost converter and the ideal internal resistance of PV array at MPP (R_{MPP}). as mentioned in [43], [45]:

$$R_L = \frac{R_{MPP}}{\left(1-d_{MPP}\right)^2} \quad (6)$$

Where, d_{mpp} symbol is the duty cycle of the converter at maximum power point (MPP) and R_{MPP} is the internal resistance, which can be calculated using eq. 7:

$$R_{MPP} = \frac{V_{MPP}}{I_{MPP}} \quad (7)$$

For the purpose of tracking the maximum power point, the boost converter's load resistance must be higher than or equal to the PV array's ideal internal resistance at *MPP* ($R_L \geq R_{MPP}$). The array is simulated under fast diverse solar illumination to specify the range values of R_{MPP}. Different levels of irradiance were selected, the higher at $G = 1000\ W/m^2$ and the lower at $G = 200\ W/m^2$ [46]. Under three different magnitudes of illumination Figures 3 and 4 show the characteristic variation of the curves I–V, P–V, and optimum internal resistance. When the radiation intensity was reduced from $1000\ W/m^2$ to $200\ W/m^2$, the MPP decreased from 249 W to 49.15 W. As a result, the R_{MPP} increased from 3.61 W to 17.75 W; thus, the load resistance

value of 53 ohm was chosen for this study to be higher than the R_{MPP} in the case of lowest illumination.

For a predefined value of load resistance and a lossless converter (P_O = Ppv). The output voltage V_O of the converter, the duty ratio D_{MPP}, and the output current Io can be calculated using equation 8,9, 204 and 10:

$$V_o = \sqrt{(P_o \times R_L)} \tag{8}$$

$$D_{MPP} = 1 - \frac{V_{pv}}{V_o} \tag{9}$$

$$I_o = \frac{P_{MPP}}{V_o} \tag{10}$$

- Selection of the inductor:

The boost convertor inductor value is selected depending on the maximum amount of appropriate current ripple at the MPP in the case of maximum solar radiation (1000W/m^2). As presented in equation 11, When the magnitude of inductor is high, the magnitude of output current ripple is low, and vice versa. In this proposed work, the switching frequency fs was set to 25 kHz in order to reduce oscillations at the MPP, and the inductor value was properly considered for input current ripple ΔIpv of 1% [46]. As a result, the inductor's minimum value was designed according to the equation 11 [46], [47]:

$$L = \frac{V_{pv} \times D_{MPP}}{2 \times \Delta I_{pv} \times f_s} \tag{11}$$

In this research, the inductor value L is chosen to be 1.1 mH to guarantee minimal current ripple at the boost converter's output, which is critical for this application

- Selection of the capacitor:

The output and input value of capacitor was calculated using the output voltage ripple ΔV_O of 2%, as following equation [47], [48], [49].

$$C = \frac{V_o \times D_{MPP}}{2 \times \Delta V_o \times R \times f_s} \tag{12}$$

In this proposed study, the input capacitor C_1 and the output capacitor C_2 are chosen to be 400 μF to ensure that we maintained the permissible voltage ripple limit for efficient MPP tracking under any radiation variations [28]. Using all the above equations, Table 1 summarizes the PV array characteristics at 25 C for higher and lower solar irradiances.

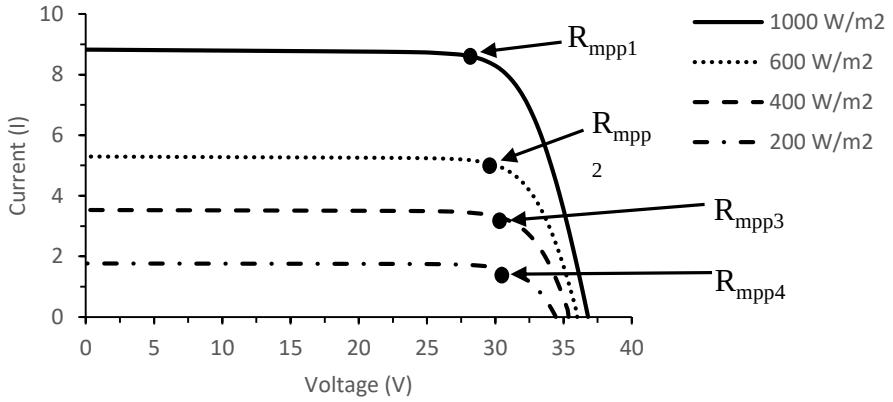

Figure 3. I–V curves of PV module at four insolation level.

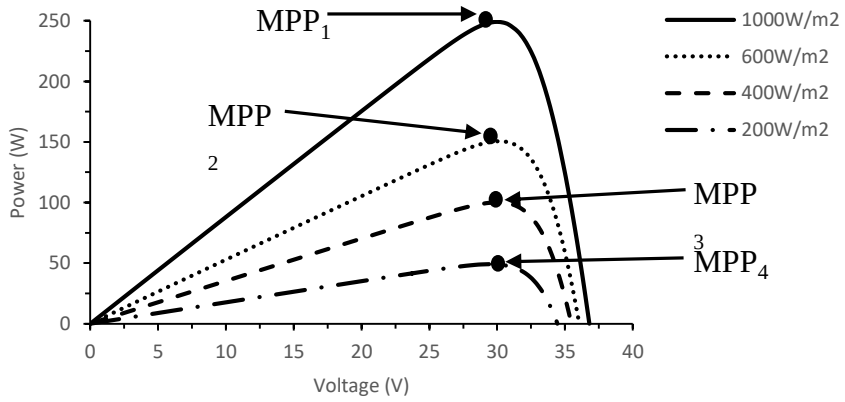

Figure 4. P–V curves of PV module at four insolation level.

Table 1. PV solar array and boost converter parameters under the lower and higher solar insolation.

Irradiance (W/m^2)	V_{mpp} (V)	I_{mpp} (A)	P_{mpp} (W)	R_{mpp} (Ω)	R_L (Ω)	L (mH)	C_1 (μF)	C_2 (μF)
1000 200	30 29.544	8.3 1.664	249 49.15	3.61 17.75	53	1.1	400	400

3. Proposed Fuzzy-based Variable Step Size P&O MPPT

3.1. P&O Algorithm

As shown in Figure 5(A), the operation of the P&O concerns shifting the PV operation point according to the sign of the last increase of PV power. Otherwise stated, as the PV power increases, the operation point increases as well and vice versa. In the end, it oscillates about the MPP with a fixed step size. The process of P&O according to solar PV under constant irradiation is shown in Figure 5(B).

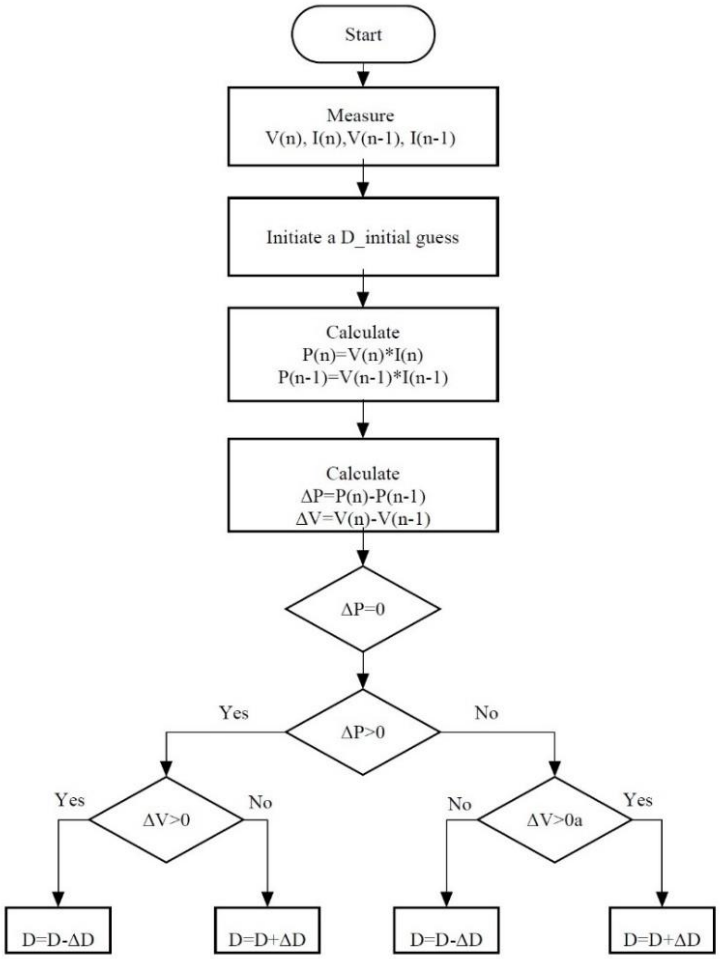

(a)

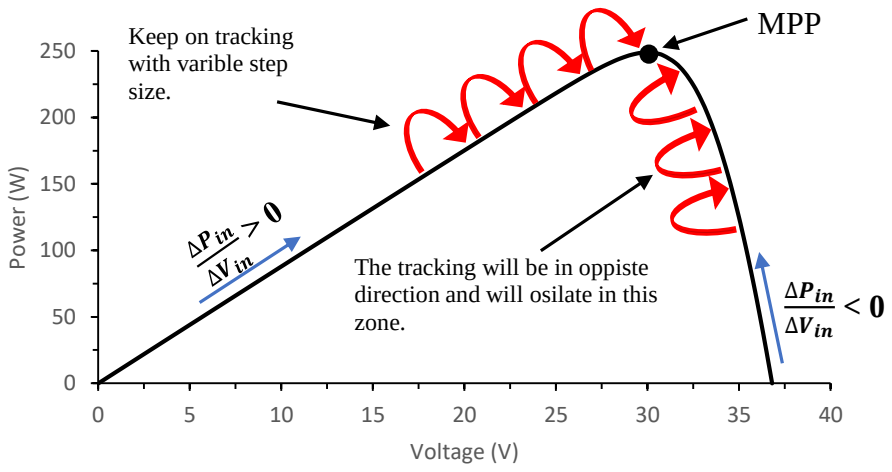

(b)

Figure 5. P&O MPPT operation (a) Flowchart for P&O (b) MPP P&O-based tracking under Constant Irradiation.

3.2. Fuzzy Algorithm

Lotfi A. Zadeh, a computer science professor at the University of California at Berkeley, pioneered fuzzy logic in 1965. FLC operates with inaccurate inputs, does not require a perfect mathematical model, and is capable of handling nonlinearity. Furthermore, as compared to traditional non-linear controllers, fuzzy is more robust. The four essential aspects of FLC operation can be classified into fuzzification, rule basis, inference engine, and defuzzification.

The basic idea behind the proposed hybrid algorithm is to combine the abilities of both the FLC and P&O algorithms into a single platform. The method is developed in two stages, the first of which uses FLC to provide an initial guess in the region of MPP to the P&O. Therefore, this integration combines the speed of FLC approximation with the accuracy of P&O. The second stage uses another FLC to find the appropriate P&O step size. When utilizing a fixed step size perturbation in a standard P&O, there is a conflict between eliminating oscillation of PV array output power near MPP and convergence of rising time approaching MPP. A large step size allows a quick dynamic response due to a sudden solar irradiance change. However, it results in excessive steady-state fluctuation of the PV array output power near MPP, resulting in power loss. A small step size ensures that PV array output power oscillates less around MPP, but it also obtains a slower dynamic response to a rapid change in solar irradiance. In order to provide small steady-state oscillations and quick dynamic response, a variable step size MPPT will be required. Therefore, FLC is used to tune the step size for P&O-based MPPT to overcome the constraints of the conventional fixed step size P&O.

3.2.1. Initial guess FLC-based

The first FLC has two inputs open circuit voltage (Voc) and short circuit current (Isc) and a single output (Initial guess of D (D_{in}), and there are five fuzzy sets in each: VS (very small), S (small), M (medium), L (large), and VL (very large), as shown in Figure 6 and Table 2.

The fuzzy rule base and fuzzy implication sub blocks compose the inference engine. The fuzzified inputs then passed to the inference engine, where the rule base is applied based on table 2. Using the fuzzy implication method, the output fuzzy set is identified. The MIN-MAX fuzzy implication is used in this study [50] . Figure 7 depicts the surface that was generated for the fuzzy controller.

Table 2. Fuzzy inference table.

Voc/Isc	VS	S	M	L	VL
VS	M	M	S	L	VL
S	M	M	M	L	VL
M	VS	S	M	L	VL
L	VS	S	M	M	M
VL	VS	S	L	M	M

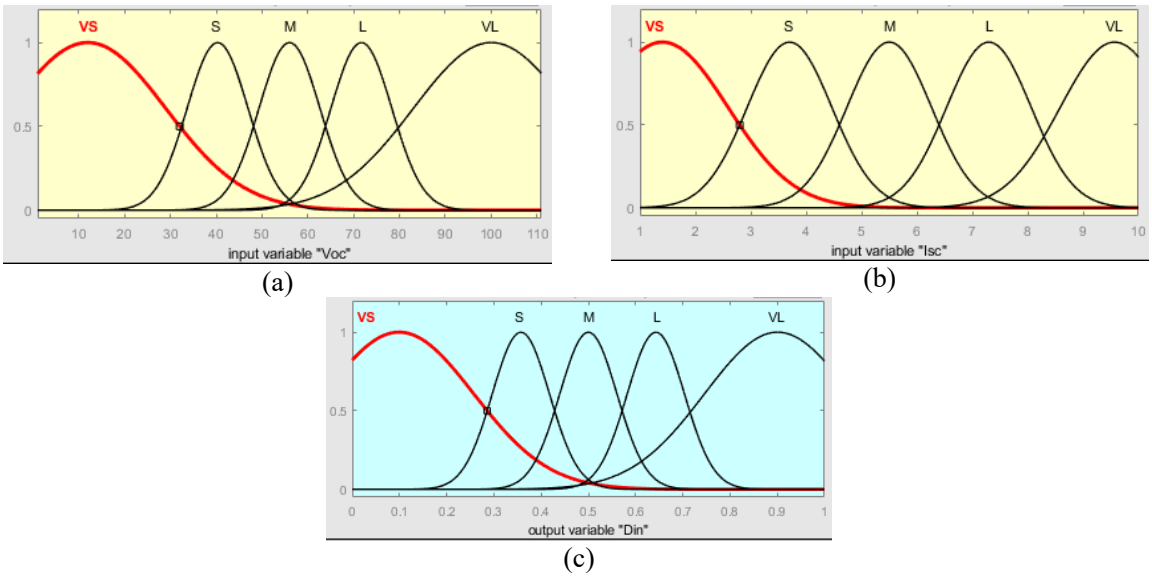

Figure 6. (a)Membership function plots for Voc, (b)Membership function plots for Isc, (c) Membership function plots for D_i

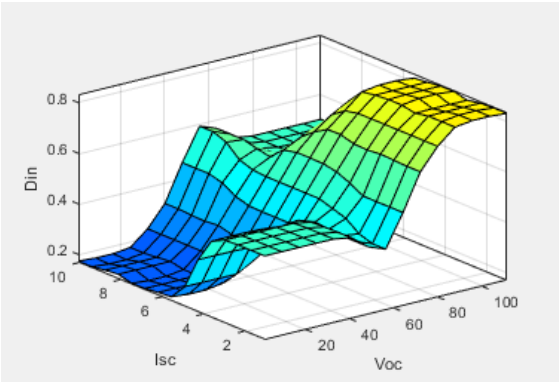

Figure 7. Surface of generated FLC.

In this stage, FLC is responsible for finding the appropriate step size of P&O. FLC has two inputs (Error (E) and change in error (CE)) The inputs are shown in Eq.s (13) and (14), where E is the P-V curve's slope that defines the MPP's position in the PV module and CE determines whether the operating point is moving in the MPP direction or not. The output is the step size of the change in duty cycle (Delta). This signal is transferred to a dc-dc converter, which is used to drive the load.

Each input includes five fuzzy sets: NL (negative large), NS (negative small), ZE (zero), PS (positive small), and PL (positive large), and the output includes five fuzzy sets: VS (very small), S (small), M (medium), L (large), and VL (very large) as shown on Table 3. As a result, the FLC has twenty-five rules based on Table 3, where these rules are based on minimizing the absolute slope of the P-V curve. The MIN-MAX fuzzy implication approach is employed. The membership functions of the inputs and outputs are shown in Figures 8 and 9 depicts the surface that was generated for the fuzzy controller.

$$E(n)=\frac{P(n)-P(n-1)}{V(n)-V(n-1)}=\frac{\Delta P}{\Delta V} \tag{13}$$

$$CE(n)=E(n)-E(n-1)=\Delta E \tag{14}$$

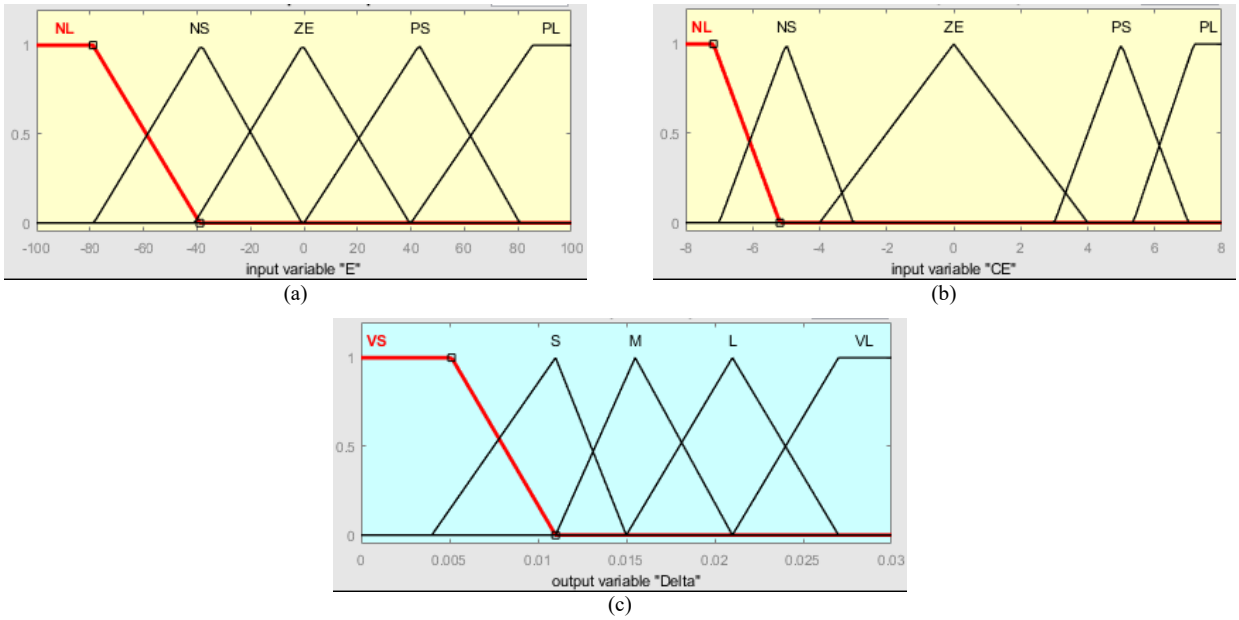

(a) (b) (c)

Figure 8. (a) Membership function plots for E (b) Membership function plots for CE (c) Membership function plots for Delta.

Table 3. Fuzzy inference table.

E/ΔE	NL	NS	ZE	PS	PL
NL	VL	NL	S	S	VS
NS	VS	VS	S	S	S
ZE	VS	VS	S	VL	S
PS	S	S	VL	VL	VL
PL	S	S	VL	VL	VL

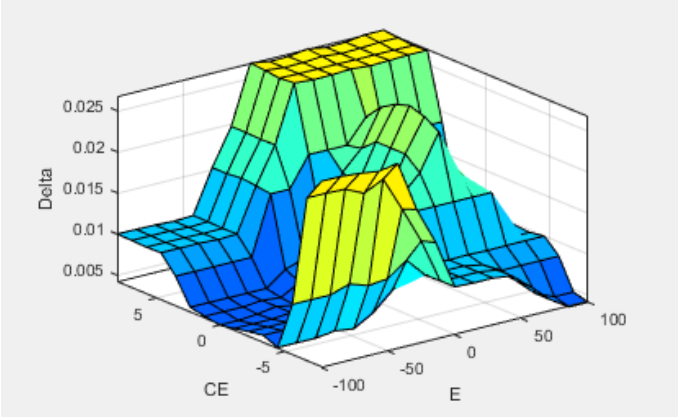

Figure 9. Surface of generated FLC.

The flowchart of the hybrid FLC-P&O-FLC controller is shown in Figure 10. The flowchart shows a hybrid control system that combines the Perturb & Observe (P&O) technique with Fuzzy Logic Control (FLC) to improve the efficiency of solar energy utilization. The fuzzy logic controller provides an initial estimate of duty cycle after the system starts by measuring voltage and current values. Power computations are then performed to determine power and voltage differences for between the present and previous states. These differences allow the duty cycle to be modified to maximize power production while minimizing steady-state oscillations and optimizing transient responses with the use of an additional fuzzy logic controller. This dual procedure makes use of the P&O method's precision for duty cycle fine-tuning and FLC's quick approximation capabilities for preliminary estimations. Expert knowledge and experimental data were combined to estimate the ranges of the membership functions for the inputs and outputs in Figures 6 and 8. The performance features of the MPPT algorithm and the typical operating conditions of PV systems were considered. This approach allows to ensure that the membership functions accurately represent the input and output variables within the framework of this study.

Overall, after merging the two stages, the first FLC ensures speedy approximation of the initial guess, the second FLC ensures steady-state oscillations and fast dynamic reaction based on a variable step size, moreover, the P&O approach ensures the accuracy of the process. Figure 11 shows a complete MATLAB/Simulink model.

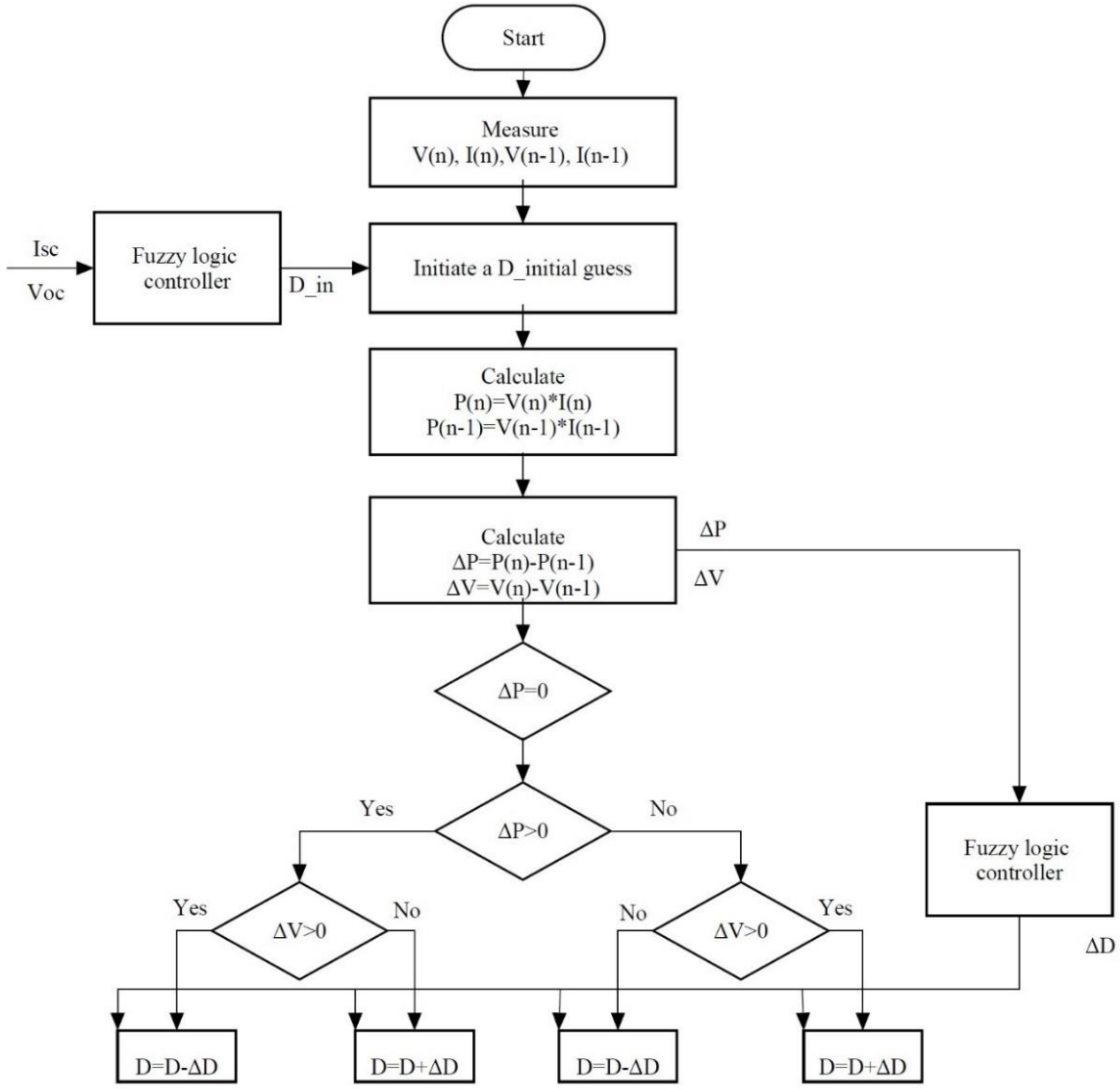

Figure 10. The hybrid FLC-P&O-FLC controller flowchart.

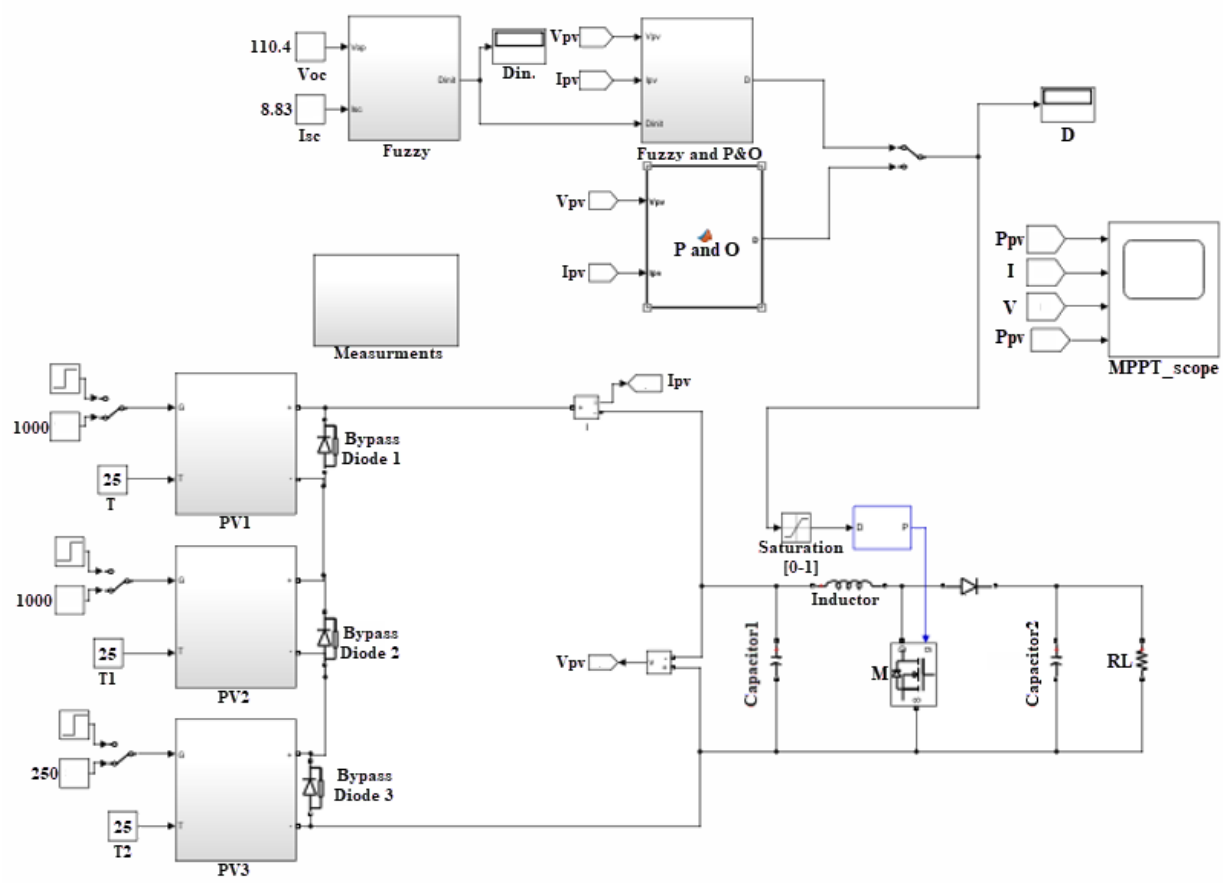

Figure 11. The hybrid FLC-P&O-FLC MATLAB simulation model.

4. Results and discussion

The performance of the proposed hybrid FLC-P&O-FLC controller variable step size MPPT controller is simulated by modeling the entire system in MATLAB/Simulink environment under any weather conditions, the system consists of a TP250MBZ PV panel operating at variable atmospheric conditions (Table 4) and a DC-DC boost converter driven by the proposed controller to provide it with the optimal duty cycle to achieve GMPP of the entire system in various cases of insolation levels. The controller tracking efficiency is evaluated from Eq. 15 [51].

$$\eta = \frac{P_o}{P_{\max}} \times 100\% \quad (15)$$

where Po is the output power of the PV solar module, that tracked by the controller and P_{max} is the maximum value of real power.

The system is studied and carried out under different weather conditions; Uniform irradiation, sudden change, and partial shading (weak, moderate, and strong) as illustrated in Figures 12 and 13.

Table 4. Electrical Characteristics of TP250MBZ module (1000 W/m², 25°C)

Designation	Values
Maximum Power (P_{MPP})	250W
Voltage Pmax (V_{MPP})	30V
Current at Pmax (I_{MPP})	8.3A
Short Circuit current (I_{sc})	8.83A
Open Circuit voltage (V_{oc})	36.8V
Temperature coefficient of V_{oc}	-0.03 %/ 0 6y c
Temperature coefficient of I_{sc}	0.063805 %/deg.°C

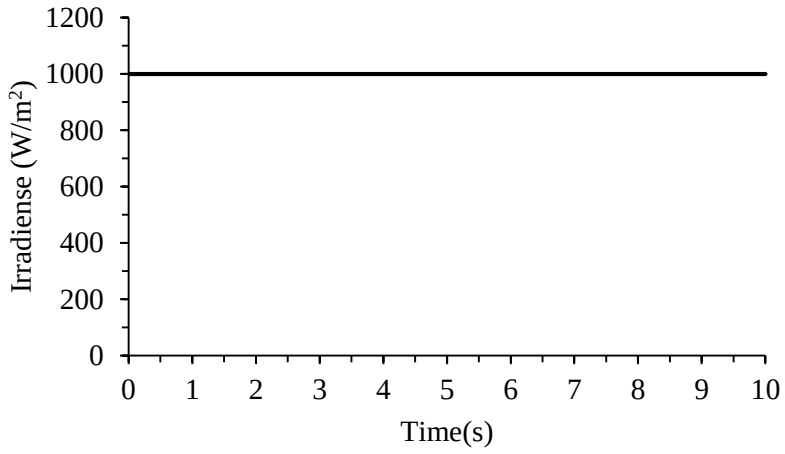

Figure 12. Uniform irradiation pattern used for the MPPT performance testing.

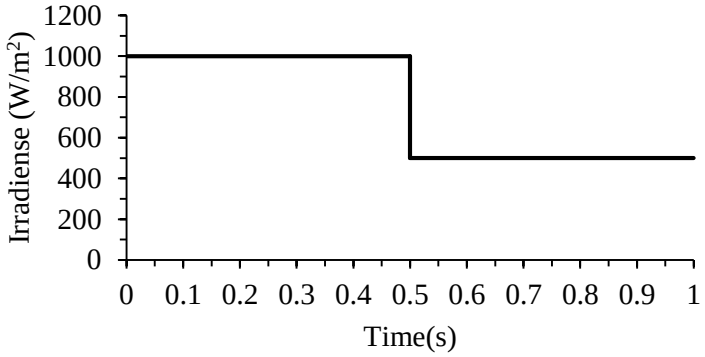

(a) Sudden drop in radiation level from 1000 W/m^2 to 500 W/m^2

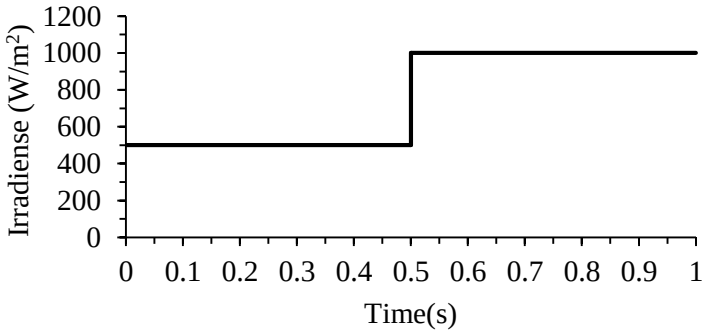

(b) Sudden rise in radiation level from 500 W/m^2 to 1000 W/m^2

Figure 13. Sudden change irradiation pattern used for the MPPT performance testing

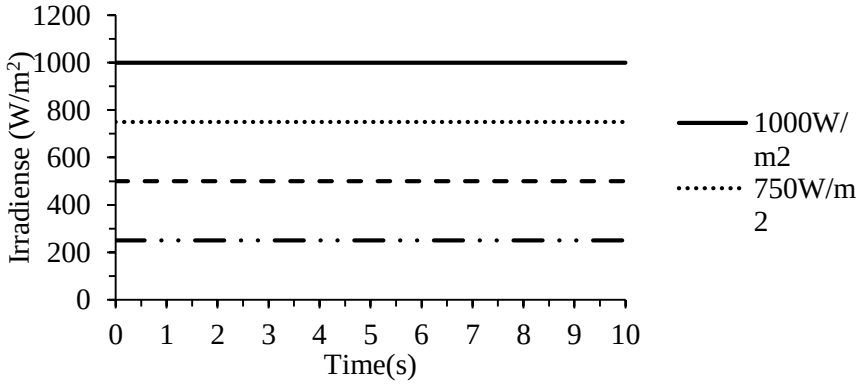

Figure 14. Partial shading patterns (weak 750 W/m^2, moderate 500 W/m^2, and strong 250 W/m^2) used for the MPPT performance testing

The comparison of the proposed FLC-P&O-FLC and the conventional P&O is done in various scenarios:

4.1. Uniform irradiation

A comparison of the performance of the P&O and the proposed FLC-P&O-FLC under a uniform irradiance is shown in Figure 15. The three PV panels receive the same amount of solar irradiance (1000 W/m^2). It can be observed that the proposed FLC-P&O-FLC reaches the MPP faster at t=0.14 s.

4.2. Sudden irradiation change

To simulate the rapidly varying irradiation condition, the irradiation level was unexpectedly reduced from 1000 W/m^2 to 500 W/m^2 and then increased from 500 W/m^2 to 1000 W/m^2. As shown in Figures 16 and 17, respectively, it is noticed that the efficiency of the proposed FLC- P&O-FLC controller is better than the efficiency of the conventional P&O.

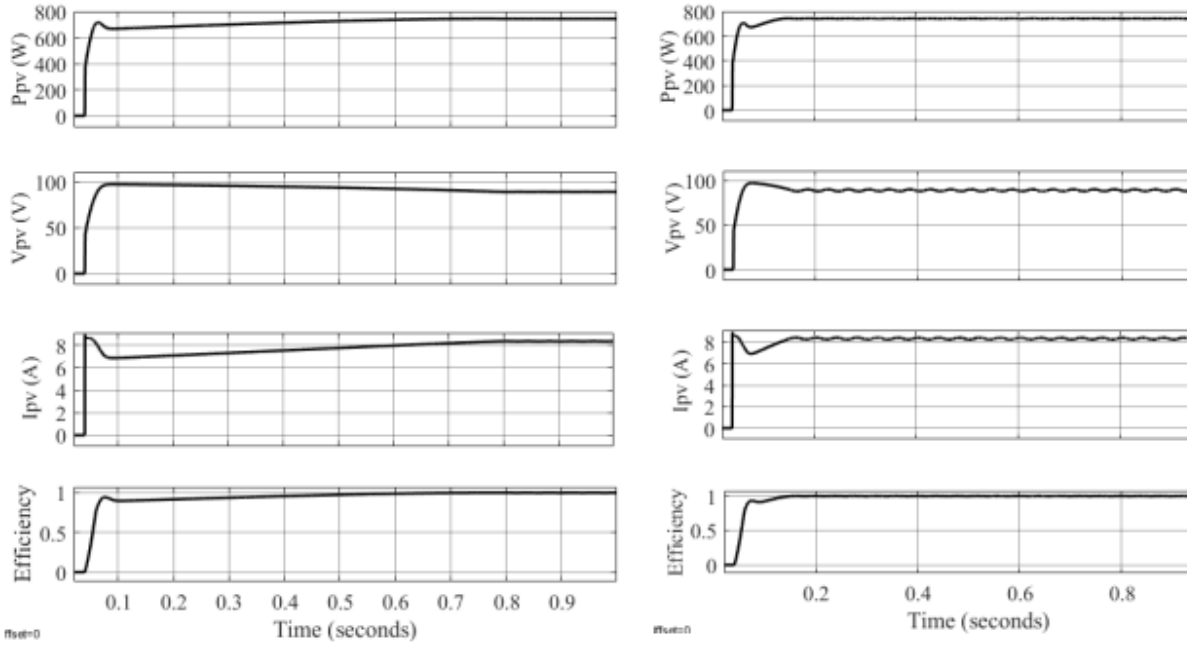

Figure 15. The simulation results of PV system under a uniform irradiance (1000 W/m^2) (a) Conventional P&O and (b) The proposed FLC-P&O-FLC controller.

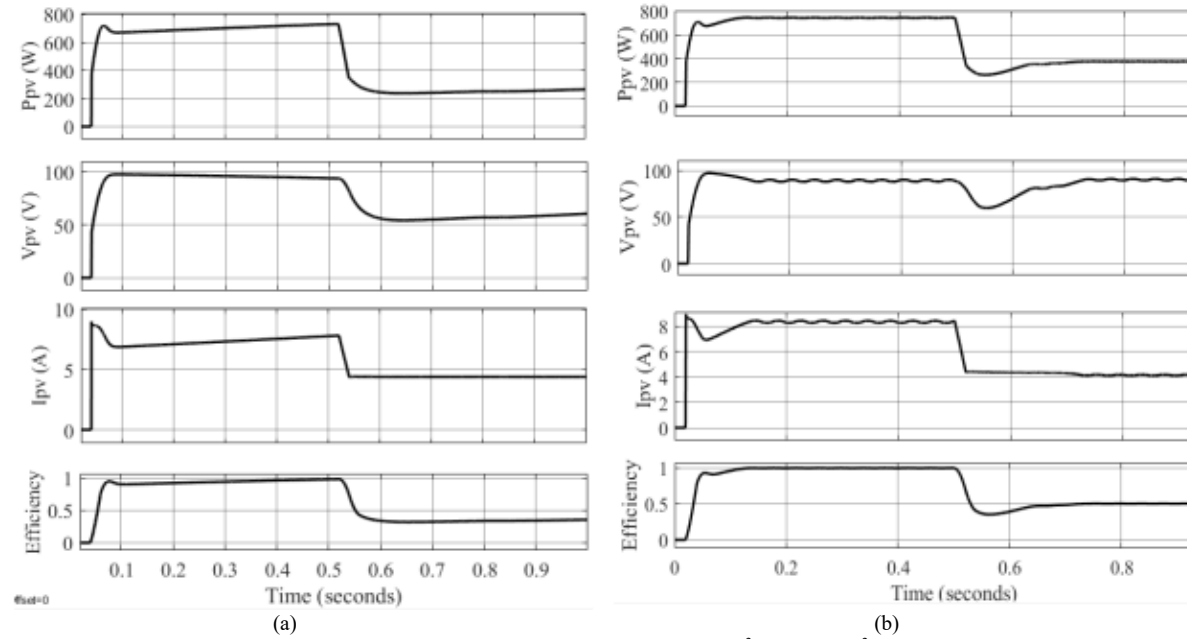

Figure 16. The simulation results of PV system under a sudden irradiance (1000 W/m^2 to 500 W/m^2) (a) conventional P&O and (b) the proposed FLC-P&O-FLC controller.

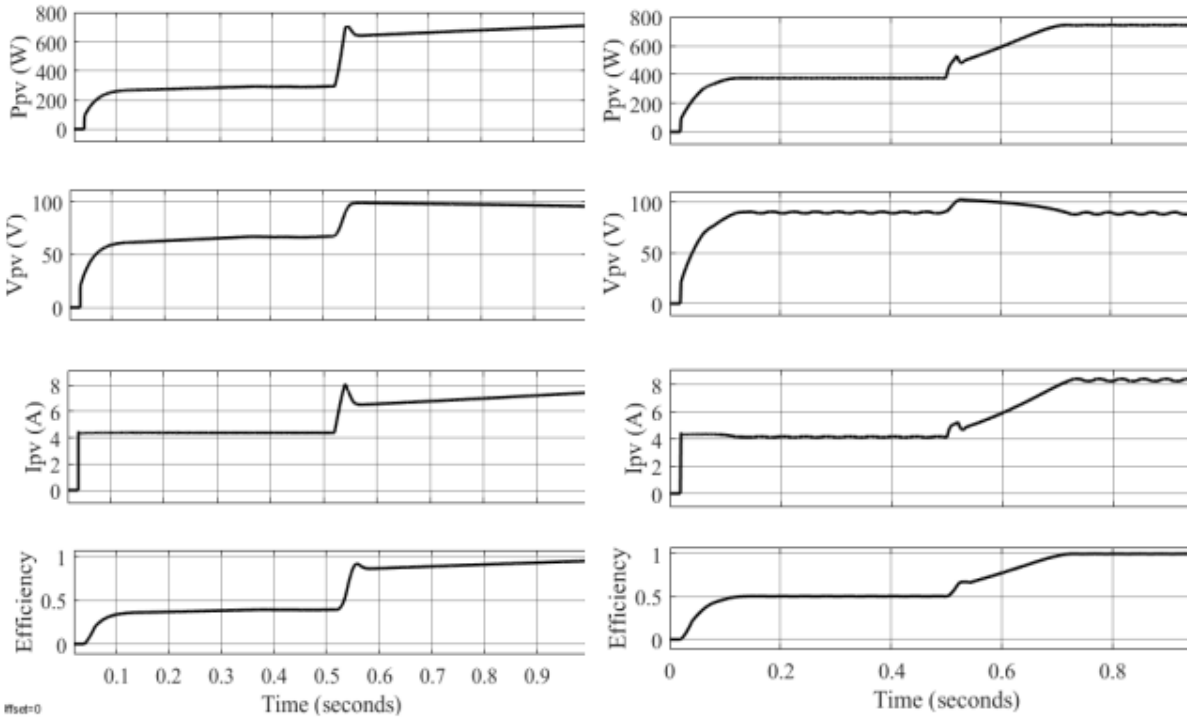

Figure 17. The simulation results of PV system under a sudden irradiance (500 W/m^2 to 1000 W/m^2) (a) Conventional P&O and (b) The proposed FLC-P&O-FLC controller.

4.3. Partial irradiation shading

Various cases of partial shading (weak, moderate, and strong) were considered in the simulation for extensive verification and to validate the effectiveness of the proposed technique. In this section, the simulation results for partial shading cases are discussed along with a performance comparison of the proposed FLC-P&O-FLC technique versus the conventional P&O technique.

4.3.1. Weak, moderate, and strong partial shading pattern

In case of weak partial shading pattern, two connected panels obtain uniform radiation (1000 W/m^2), while one receives 750 W/m^2. The arrangement of this case and all partial shading cases are listed in Table 5. Figure 18 shows the output characteristic of P–V curve of the PV generator for partial shading cases, two peaks maximum power are noted referring respectively to GMPP and local maximum power point (LMPP).

Through the time under study, the proposed FLC-P&O-FLC technique has the ability to differentiate GMPP and LMPP. Furthermore, as depicted in Figures 19-21, the proposed FLC-P&O-FLC technique can track the GMPP, and it still has a rapid response time even under partial irradiation shading and successfully locates the global maximum power point while the P&O got trapped in the LMPP. The fuzzy controller always discovers the duty cycle that gets the system close to the GMPP. The P&O algorithm part of the proposed FLC-P&O-FLC technique uses this duty cycle which is used as an initial guess in order to increase the power obtained by the PV module.

Table 5. Incident insolation for the PV system array with the corresponding power at the global maximum power point (GMPP).

Case	Irradiation on the solar module (W/m^2)	Power (W)
Strong partial shading pattern	[1000,1000,250]	577.7
Moderate partial shading pattern	[1000,1000,500]	577.9
Weak partial shading pattern	[1000,1000,750]	657.1

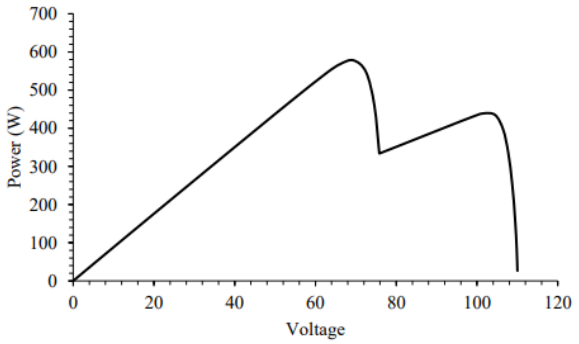

Figure 18. output characteristic of P–V curve for partial moderate shading case.

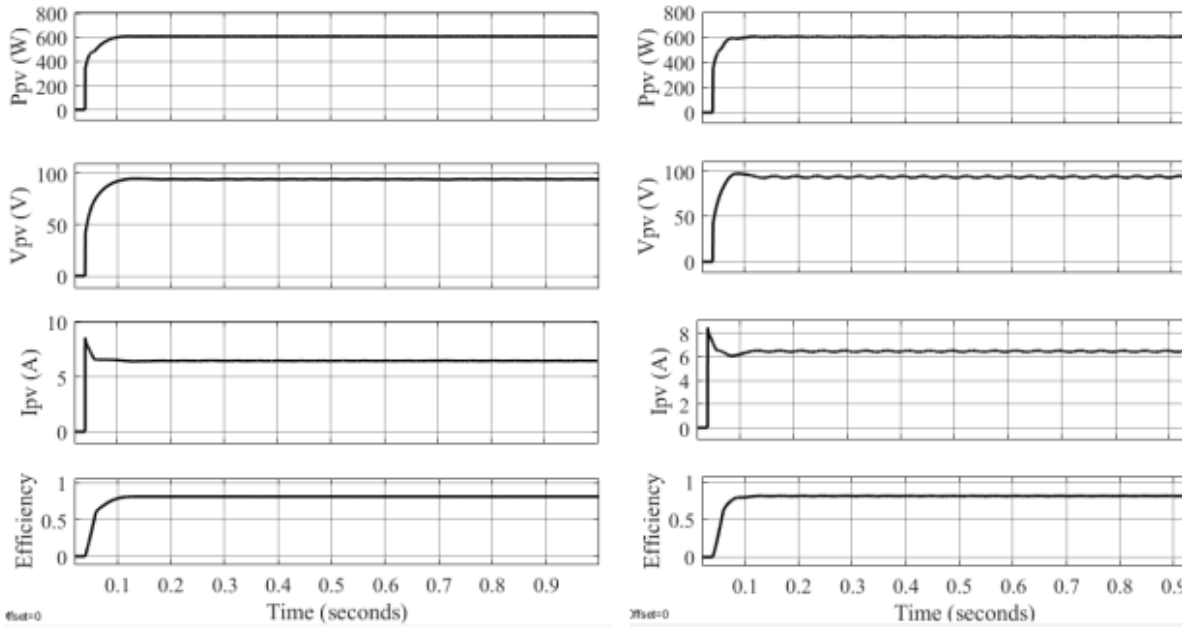

(a) (b)

Figure 19. The simulation results of PV system under a weak partial shading irradiance. (a) Conventional P&O and (b) The proposed FLC-P&O-FLC controller.

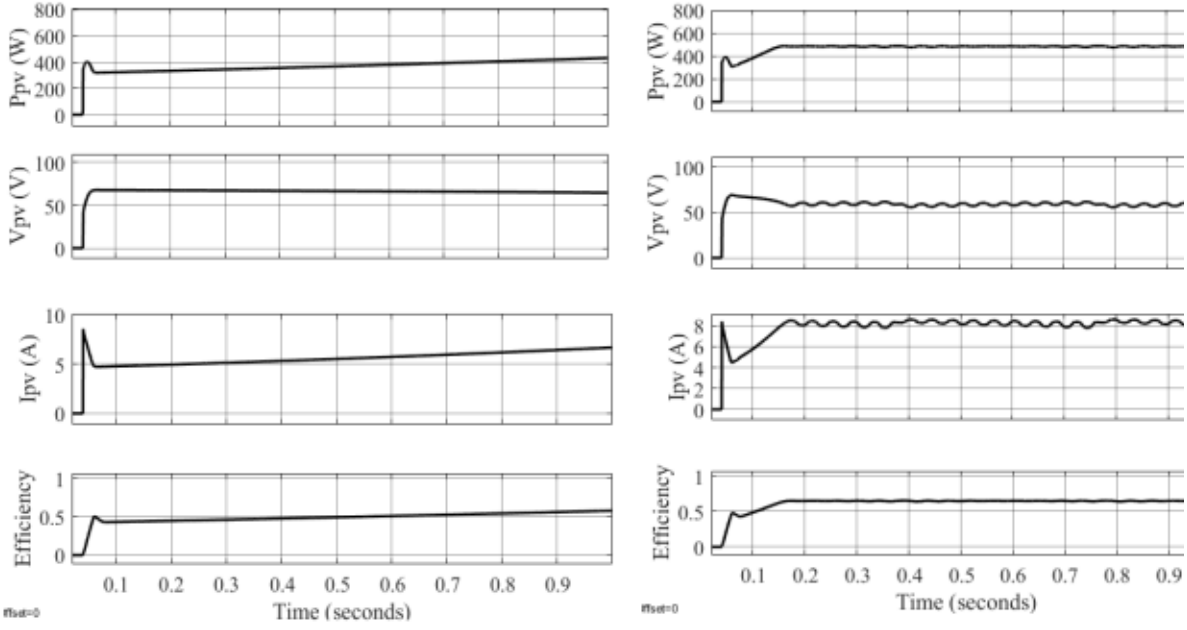

(a) (b)

Figure 20. The simulation results of PV system under a moderate partial shading irradiance. (a) Conventional P&O and (b) The proposed FLC-P&O-FLC controller.

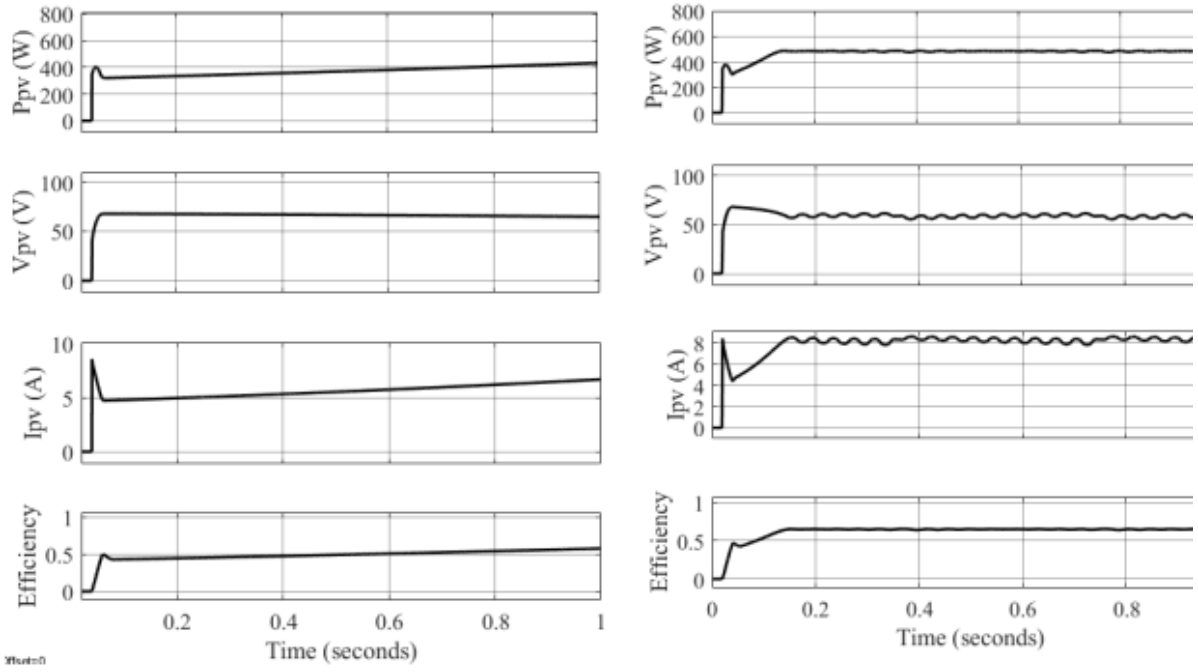

Figure 21. The simulation results of PV system under a strong partial shading irradiance. (a) Conventional P&O and (b) The proposed FLC-P&O-FLC controller.

A performance comparison under various conditions of conventional P&O and the proposed FLC- P&O-FLC controller is shown in Table 6.

Table 6. A performance comparison under various conditions of conventional P&O and the proposed FLC-P&O-FLC controller

Parameter	**Conventional P&O [52], [53]**	**FLC-P&O-FLC**
Tracking speed	Good	Very Good
Steady state error	High	Medium
Reaching true MPP	No	Yes
Oscillations	Low	Medium

5. Conclusion

The basic idea behind the proposed hybrid controller is to combine the abilities of both the FLC and P&O algorithms into a single platform. The method is developed in two stages, the first of which uses FLC to provide an initial guess in the region of MPP to the P&O. Therefore, this integration combines the speed of FLC approximation with the accuracy of P&O. The second stage uses another FLC to find the appropriate P&O step size. When utilizing a fixed step size perturbation in a standard P&O, there is a conflict between eliminating oscillation of PV array output power near MPP and convergence of rising time approaching MPP. A large step size allows a quick dynamic response due to a sudden solar irradiance change. However, it results in excessive steady-state fluctuation of the PV array output power near MPP, resulting in power loss. A small step size ensures that PV array output power oscillates less around MPP, but it also obtains a slower dynamic response to a rapid change in solar irradiance. In order to provide small steady-state oscillations and quick dynamic response, a variable step size MPPT is proposed. Therefore, FLC is used to tune the step size for P&O-based MPPT to overcome the constraints of the conventional fixed step size P&O. The robustness and effectiveness of the proposed controller were illustrated under various weather conditions simulation results, the accuracy was improved, and the efficiency was enhanced, the tracking efficiency for the conventional P&O and the proposed FLC-P&O-FLC controller have a difference of 0.30% in favor of the FLC-P&O-FLC controller.

6. Future work

In future work, we will confirm the proposed algorithm's performance experimentally. It would also be an interesting goal to test its validity on other converter structures.

References

[1] O. Badran, E. Abdulhadi, R. Mamlook, "Evaluation of solar electric power technologies in Jordan," *Jordan Journal of Mechanical and Industrial Engineering*, vol. 4, no. 1, 2010.

[2] Q. A. Khasawneh, Q. A. Damra, O. H. Bany Salman, "Determining the Optimum Tilt Angle for Solar Applications in Northern Jordan," *Jordan Journal of Mechanical and Industrial Engineering*, vol. 9, no. 3, 2015.

[3] M. Abdelkader, A. Al-Salaymeh, Z. Al-Hamamre, F. Sharaf, "A comparative Analysis of the Performance of Monocrystalline and Multiycrystalline PV Cells in Semi Arid

Climate Conditions: the Case of Jordan," *Jordan Journal of Mechanical and Industrial Engineering*, vol. 4, no. 5, 2010.

[4] M. Al Zou'bi, "Renewable energy potential and characteristics in Jordan," *Jordan Journal of Mechanical and Industrial Engineering*, vol. 4, no. 1, 2010, pp. 45-48.

[5] M. Hamdan, M. Shehadeh, A. Al Aboushi, A. Hamdan, E. Abdelhafez, "Photovoltaic Cooling Using Phase Change Material," *Jordan Journal of Mechanical and Industrial Engineering*, vol. 12, no. 3, 2018.

[6] Y. M. Al-Smadi *et al.*, "Assessment and Perception of Renewable Energy Awareness and Potential in Jordan," *Jordan Journal of Mechanical and Industrial Engineering*, vol. 16, no. 4, 2022.

[7] G. M. Tashtoush,M. A. Alzoubi, "An analysis of the Performance and Economic Feasibility of a Hybrid Solar Cooling System that Combines an Ejector with Vapor Compression Cycles, Powered by a Photovoltaic Thermal (PV/T) Unit," *Jordan Journal of Mechanical and Industrial Engineering*, vol. 17, no. 1, 2023, https://doi.org/10.59038/jjmie/170104

[8] D. Rekioua,E. Matagne, *Optimization of photovoltaic power systems: modelization, simulation and control*. Springer Science & Business Media, 2012.

[9] A. N. Mahmod Mohammad, M. A. Mohd Radzi, N. Azis, S. Shafie, M. A. Atiqi Mohd Zainuri, "An enhanced adaptive perturb and observe technique for efficient maximum power point tracking under partial shading conditions," *Applied Sciences*, vol. 10, no. 11, 2020, p. 3912,https://doi.org/10.3390/app10113912

[10] L. Piegari, R. Rizzo, I. Spina, P. Tricoli, "Optimized adaptive perturb and observe maximum power point tracking control for photovoltaic generation," *Energies*, vol. 8, no. 5, 2015, pp. 3418-3436,https://doi.org/10.3390/en8053418

[11] C. Li, Y. Chen, D. Zhou, J. Liu, J. Zeng, "A high-performance adaptive incremental conductance MPPT algorithm for photovoltaic systems," *Energies*, vol. 9, no. 4, 2016, p. 288,https://doi.org/10.3390/en9040288

[12] D. Baimel, R. Shkoury, L. Elbaz, S. Tapuchi, N. Baimel, "Novel optimized method for maximum power point tracking in PV systems using Fractional Open Circuit Voltage technique," *2016 International Symposium on Power Electronics, Electrical Drives, Automation and Motion (SPEEDAM)*, 2016

[13] B. Büyükgüzel,M. Aksoy, "A current-based simple analog MPPT circuit for PV systems," *Turkish Journal of Electrical Engineering and Computer Sciences*, vol. 24, no. 5, 2016, pp. 3621-3637,https://doi.org/10.3906/elk-1407-21

[14] V. Jately, B. Azzopardi, J. Joshi, A. Sharma, S. Arora, "Experimental Analysis of hill-climbing MPPT algorithms under low irradiance levels," *Renewable and Sustainable Energy Reviews*, vol. 150, 2021, p. 111467,https://doi.org/10.1016/j.rser.2021.111467

[15] B. Abd Essalam,K. Mabrouk, "Development of a bond graph control maximum power point tracker for photovoltaic: theoretical and experimental," *JJMIE*, vol. 7, no. 1, 2013.

[16] E. K. Anto, J. A. Asumadu, P. Y. Okyere, "PID-based P&O MPPT controller for offgrid solar PV systems using Ziegler-Nichols tuning method to step, ramp and impulse inputs," *Journal of Multidisciplinary Engineering Science Studies (JMESS)*, vol. 2, no. 7, 2016, pp. 669-680.

[17] J. Sahoo, S. Samanta, S. Bhattacharyya, "Adaptive PID controller with P&O MPPT algorithm for photovoltaic system," *IETE Journal of research*, vol. 66, no. 4, 2020, pp. 442-453,https://doi.org/10.1080/03772063.2018.1497552

[18] C. Kamalakannan, L. P. Suresh, S. S. Dash, B. K. Panigrahi, "Power Electronics and Renewable Energy Systems Proceedings of ICPERES 2014," *Proceedings of ICPERES*, 2014, p. 1.

[19] C. Napole, M. Derbeli, O. Barambones, "Fuzzy logic approach for maximum power point tracking implemented in a real time photovoltaic system," *Applied Sciences*, vol. 11, no. 13, 2021, p. 5927,https://doi.org/10.3390/app11135927

[20] H. Bounechba, A. Bouzid, K. Nabti, H. Benalla, "Comparison of perturb & observe and fuzzy logic in maximum power point tracker for PV systems," *Energy Procedia*, vol. 50, 2014, pp. 677-684,https://doi.org/10.1016/j.egypro.2014.06.083

[21] M. S. Bouakkaz, A. Boukadoum, O. Boudebbouz, I. Attoui, N. Boutasseta, A. Bouraiou, "Fuzzy logic based adaptive step hill climbing MPPT algorithm for PV energy generation systems," *2020 International conference on computing and information technology (ICCIT-1441)*, 2020

[22] C. G. Villegas-Mier, J. Rodriguez-Resendiz, J. M. Álvarez-Alvarado, H. Rodriguez-Resendiz, A. M. Herrera-Navarro, O. Rodríguez-Abreo, "Artificial neural networks in MPPT algorithms for optimization of photovoltaic power systems: A review," *Micromachines*, vol. 12, no. 10, 2021, p. 1260,https://doi.org/10.3390/mi12101260

[23] A. Alkhatatbeh, M. A. Gharaibeh, R. Al-Jarrah, A. M. Jawarneh, "Artificial Neural Networks Modeling of the Electricity Demands in the Jordanian Industrial Sector," *Jordan Journal of Mechanical and Industrial Engineering*, vol. 81, no. 2, 2024, https://doi.org/10.59038/jjmie/180204

[24] Y.-T. Chen, Y.-C. Jhang, R.-H. Liang, "A fuzzy-logic based auto-scaling variable step-size MPPT method for PV systems," *Solar Energy*, vol. 126, 2016, pp. 53-63,https://doi.org/10.1016/j.solener.2016.01.007

[25] M. Farhat, O. Barambones, L. Sbita, J. G. de Durana, "A stable FLC-based MPPT technique for photovoltaic system," *2015 IEEE International Conference on Industrial Technology (ICIT)*, 2015

[26] S. Hadji, J.-P. Gaubert, F. Krim, "Real-time genetic algorithms-based MPPT: study and comparison (theoretical an experimental) with conventional methods," *Energies*, vol. 11, no. 2, 2018, p. 459,https://doi.org/10.3390/en11020459

[27] K.-H. Chao,M. N. Rizal, "A hybrid MPPT controller based on the genetic algorithm and ant colony optimization for photovoltaic systems under partially shaded conditions," *Energies*, vol. 14, no. 10, 2021, p. 2902,https://doi.org/10.3390/en14102902

[28] M. Alshareef, Z. Lin, M. Ma, W. Cao, "Accelerated particle swarm optimization for photovoltaic maximum power point tracking under partial shading conditions," *Energies*, vol. 12, no. 4, 2019, p. 623,https://doi.org/10.3390/en12040623

[29] C. González-Castaño, C. Restrepo, S. Kouro, J. Rodriguez, "MPPT algorithm based on artificial bee colony for PV system," *Ieee Access*, vol. 9, 2021, pp. 43121-43133,https://doi.org/10.1109/access.2021.3066281

[30] D. Remoaldo,I. Jesus, "Analysis of a traditional and a fuzzy logic enhanced perturb and observe algorithm for the MPPT of a photovoltaic system," *Algorithms*, vol. 14, no. 1, 2021, p. 24,https://doi.org/10.3390/a14010024

[31] A. K. Abdelsalam, A. M. Massoud, S. Ahmed, P. N. Enjeti, "High-performance adaptive perturb and observe MPPT technique for photovoltaic-based microgrids," *IEEE Transactions on power electronics*, vol. 26, no. 4, 2011, pp. 1010-1021,https://doi.org/10.1109/TPEL.2011.2106221

[32] M. Abdalla,T. Al-Jarrah, "Fuzzy logic control of an electrical traction elevator," *JJMIE: Jordan Journal of Mechanical and Industrial Engineering*, 2011, pp. 97-106.

[33] Y. He, "The Electric Vehicle Torque Adaptive Drive Anti-Skid Control Based on Objective Optimization," *Jordan Journal of Mechanical and Industrial Engineering*, vol. 15, no. 1, 2021.

[34] Z. You, "Fault Tolerant Control Method of Power System of Tram Based on PLC," *Jordan Journal of Mechanical and Industrial Engineering*, vol. 15, no. 1, 2021.

[35] B. Wei,H. Jiao, "Fault Status Information Monitoring Technology for Large Complex Electromechanical System," *Jordan Journal of Mechanical and Industrial Engineering*, vol. 15, no. 1, 2021.

[36] R. Arulmurugan,N. S. Vanitha, "An Intelligent novel FLC based FOINC MPPT technique for PV applications," *2014 International Conference on Advances in Electrical Engineering (ICAEE)*, 2014

[37] J. Macaulay,Z. Zhou, "A fuzzy logical-based variable step size P&O MPPT algorithm for photovoltaic system," *Energies*, vol. 11, no. 6, 2018, p. 1340,https://doi.org/10.3390/ en11061340

[38] H. M. Al-Masri, S. K. Magableh, A. Abuelrub, O. Saadeh, M. Ehsani, "Impact of different photovoltaic models on the design of a combined solar array and pumped hydro storage system," *Applied Sciences*, vol. 10, no. 10, 2020, p. 3650,https://doi.org/ 10.3390/ app10103650

[39] V. Vyas, D. Jani, P. Brahmbhatt, "A comprehensive study on application of renewable solar energy in thermal power generation," *National Conference on Emerging Research Trends in Engineering (NCERTE-2016), VGEC Chandkheda, Institute for Plasma Research (IPR) and CTE Gandhinagar, Ahmedabad, Apr*, 2016

[40] P. Rajput, G. Tiwari, O. Sastry, B. Bora, V. Sharma, "Degradation of mono-crystalline photovoltaic modules after 22 years of outdoor exposure in the composite climate of India," *Solar Energy*, vol. 135, 2016, pp. 786-795,https://doi.org/10.1016/j.solener.2016.06.047

[41] V. Vyas,D. Jani, "An overview on application of solar thermal power generation," *International Journal of Engineering Research and Allied Sciences*, vol. 1, 2016, pp. 1-5.

[42] F. Mayssa,S. Lassaad, "ANFIS Controlled Solar Pumping System," *i-Manager's Journal on Electronics Engineering*, vol. 1, no. 3, 2011, p. 1,https://doi.org/10.26634/jele.1.3.1419

[43] B. Nayak, A. Mohapatra, K. B. Mohanty, "Selection criteria of dc-dc converter and control variable for MPPT of PV system utilized in heating and cooking applications," *Cogent Engineering*, vol. 4, no. 1, 2017, p. 1363357,https://doi.org/ 10.1080/23311916.2017.1363357

[44] A. Hayat, A. Faisal, M. Y. Javed, M. Hasseb, R. A. Rana, "Effects of input capacitor (cin) of boost converter for photovoltaic system," *2016 International conference on computing, electronic and electrical engineering (ICE Cube)*, 2016

[45] N. Hashim, Z. Salam, D. Johari, N. F. N. Ismail, "DC-DC boost converter design for fast and accurate MPPT algorithms in stand-alone photovoltaic system," *International Journal of Power Electronics and Drive Systems*, vol. 9, no. 3, 2018, p. 1038,https://doi.org/10.11591/ijpeds.v9.i3.pp1038-1050

[46] K. Ishaque,Z. Salam, "A comprehensive MATLAB Simulink PV system simulator with partial shading capability based on two-diode model," *Solar energy*, vol. 85, no. 9, 2011, pp. 2217-2227.

[47] S. K. Kollimalla,M. K. Mishra, "A novel adaptive P&O MPPT algorithm considering sudden changes in the irradiance," *IEEE Transactions on Energy conversion*, vol. 29, no. 3, 2014, pp. 602-610,https://doi.org/10.1109/tec.2014.2320930

[48] L. P. Jyothy,M. Sindhu, "An artificial neural network based MPPT algorithm for solar PV system," *2018 4th International Conference on Electrical Energy Systems (ICEES)*, 2018

[49] T. Bennett, A. Zilouchian, R. Messenger, "A proposed maximum power point tracking algorithm based on a new testing standard," *Solar Energy*, vol. 89, 2013, pp. 23-41,https://doi.org/10.1016/j.solener.2012.11.022

[50] Y. Soufi, M. Bechouat, S. Kahla, K. Bouallegue, "Maximum power point tracking using fuzzy logic control for photovoltaic system," *2014 International conference on renewable energy research and application (ICRERA)*, 2014

[51] A. A. Allataifeh, K. Bataineh, M. Al-Khedher, "Maximum power point tracking using fuzzy logic controller under partial conditions," *Smart Grid and Renewable Energy*, vol. 6, no. 01, 2015, p. 1,https://doi.org/10.4236/sgre.2015.61001

[52] J. Ahmed,Z. Salam, "A modified P&O maximum power point tracking method with reduced steady-state oscillation and improved tracking efficiency," *IEEE Transactions on Sustainable Energy*, vol. 7, no. 4, 2016, pp. 1506-1515,https://doi.org/10.1109/tste.2016.2568043

[53] G. RajaSekhar,B. Basavaraja, "Solar PV fed non-isolated DC-DC converter for BLDC motor drive with speed control," *IJEECS*, vol. 13, no. 1, 2019, https://doi.org/10.11591/ijeecs. v13.i1.pp313-323